ISSN 0915-633X

NATIONAL INSTITUTE FOR FUSION SCIENCE

Collisionality Dependence of Mercier Stability in LHD Equilibria with Bootstrap Currents

K. Ichiguchi

(Received - Dec. 27, 1996)

NIFS-482 Feb. 1997

RESEARCH REPORT
NIFS Series

NAGOYA, JAPAN

Collisionality Dependence of Mercier Stability in LHD Equilibria with Bootstrap Currents

Katsuji Ichiguchi

National Institute for Fusion Science,

Nagoya 464-01, Japan

Abstract

The Mercier stability of the plasmas carrying bootstrap currents with different plasma collisionality is studied in the Large Helical Device (LHD). In the LHD configuration, the direction of the bootstrap current depends on the collisionality of the plasma through the change in the sign of the geometrical factor. When the beta value is raised by increasing the density of the plasma with a fixed low temperature, the plasma becomes more collisional and the collisionality approaches the plateau regime. In this case, the bootstrap current can flow in the direction so as to decrease the rotational transform. Then, the large Shafranov shift enhances the magnetic well and the magnetic shear, and therefore, the Mercier stability is improved. On the other hand, when the beta value is raised by increasing the temperature of the plasma with a fixed low density, the plasma collisionality becomes reduced to enter the $1/\nu$ collisionality regime and the bootstrap current flows so that the rotational transform should be increased, which is unfavorable for the Mercier stability. Hence, the beta value should be raised by increasing the density rather than the temperature in order to obtain a high beta plasma.

Key Words ;

Heliotron/Torsatron, MHD, Mercier stability, bootstrap current, geometrical factor, collisionality of plasma.

1 Introduction

Although a Heliotron/Torsatron configuration has an advantage that there exists a currentless magnetohydrodynamic (MHD) equilibrium, the neoclassical transport theory shows that net toroidal current such as the bootstrap current and the beam current can flow[1, 2, 3, 4]. The net toroidal current affects the MHD properties because it changes the profile of the rotational transform through the generation of the additional poloidal magnetic field. Ichiguchi et al.[5] studied the dependence of the Mercier stability[6, 7] on the net toroidal currents in the Large Helical Device (LHD) [8, 9]. They showed that the stability strongly depends on the direction of the net toroidal current of which profile is peaked at the magnetic axis. The current which flows so that the rotational transform should be decreased has a stabilizing contribution to the Mercier mode, while the current flowing in the opposite direction has a destabilizing contribution.

Watanabe et al.[10] calculated the three-dimensional (3D) MHD equilibrium including the self-consistent bootstrap currents by iterating the equilibrium calculation with the VMEC code[11] and the evaluation of the bootstrap current with the analytic expression based on the neoclassical theory. They studied the dependence of the bootstrap current in the LHD plasmas on the change of the geometry in the magnetic configurations under the assumption that the collisionality of the plasma is in the $1/\nu$ regime. In this case, the bootstrap current flows in the direction so as to increase the rotational transform, which would be unfavorable with respect to the Mercier stability.

The analytic expression of the bootstrap current can be obtained asymptotically in each limit of the plasma collisionality. In this case, the direction of the bootstrap current is almost determined by the sign of the geometrical factor which reflects the geometrical property of the particle orbit. In asymmetric configurations such as LHD, the geometrical factor has different expression depending on the collisionality. As shown in the following chapter, in the vacuum configuration of the LHD, the asymptotic value of the geometrical factor in the $1/\nu$ regime is positive, while that in the limit of the plateau regime is almost negative. Therefore, if we make the plasma more collisional so that the collisionality should approach the plateau regime, it can be expected that the direction of the bootstrap current

reverses. Thus, we consider the possibility of the reverse in the direction of the bootstrap current by changing the collisionality of the plasma in order to obtain stable high beta equilibria against the Mercier modes in the LHD configuration

Watanabe et al.[14] also studied the effects of the collisionality of the plasma by incorporating a connection formula for the estimation of the products of the geometrical factor and the viscosity coefficients in order to calculate the bootstrap currents in the plasma with any collisionality from the $1/\nu$ to the Pfirsch-Schlüter regimes. They showed the reduction of the bootstrap current with enhancement of the collisionality of the plasma. However, the current still grows in the direction so as to increase the rotational transform as the beta value increases, because they raised the beta value by the enhancement of the temperature. Hence, the Mercier mode would be still destabilized in their case. Here, we consider following two equilibrium sequences, by using the method developed by Watanabe et al. including the connection formula[14] to find stable equilibria with the bootstrap current. One is called density sequence, where the beta value is raised by increasing density with the temperature fixed. In this case, the plasma can be expected to become more collisional to reverse the direction of the bootstrap current at high beta value. The other is called temperature sequence as a reference, where the beta value is raised by increasing temperature with the density fixed. In this case, the plasma becomes less collisional.

In Section 2, the conditions used in our calculation are presented. The behavior of the bootstrap currents in the two sequences is also discussed based on the change in the geometrical factors. In Section 3, the property of the MHD equilibria in the above two sequences are shown, and the relation between the direction of the bootstrap currents and the Mercier stability of the equilibria is discussed. Concluding remarks are given in Section 4.

2 Collisionality Effects on Bootstrap Current

We calculated the equilibria consistent with the bootstrap current by utilizing the method developed by Watanabe et al.[10, 14]. In the present study, we assume that the plasma is composed of only electrons and protons and they have the same temperature, T, and the

density, n. In this case, the asymptotic expression of the total bootstrap current, I_b, in the limits of the $1/\nu$, the plateau and the Pfirsch-Schlüter collisionality regimes can be given by

$$I_b = 2\pi \int d\psi \frac{\langle \boldsymbol{J}_b \cdot \boldsymbol{B} \rangle}{\langle \boldsymbol{B}^2 \rangle}, \tag{2.1}$$

$$\langle \boldsymbol{J}_b \cdot \boldsymbol{B} \rangle = -G_b \left(L_1 \frac{dP}{d\psi} + L_2 n \frac{dT}{d\psi} \right), \tag{2.2}$$

where P and $2\pi\psi$ denote the plasma pressure and the toroidal magnetic flux, respectively. Since we assume that the electrons and the ions have the same T and n, the contribution of the radial electric field to the bootstrap current vanishes[12]. $L_j (j = 1, 2)$ are transport coefficients which consist of the viscosity and the friction coefficients, and depend on the collisionality regime of the plasma. G_b, which is called geometrical factor, plays an important role in eq.(2.2), because it determines the direction of the viscosity damp of the neoclassical flow. The bootstrap current is generated by the parallel component of the flow to the magnetic field which is needed to construct the resultant neoclassical flow together with the perpendicular flow. Therefore, the bootstrap current can change the direction depending on G_b.

In the configurations with topological symmetry, the geometrical factor is independent of the collisionality of the plasma. For example, the factor for tokamaks, G_b^{tok}, is given by J/ι, where ι denotes the rotational transform and $2\pi J$ is the total poloidal current outside of the flux surface. On the other hand, the geometrical factor in asymmetric configuration depends on not only the magnetic structure of the configuration but also the collisionality of the particles, because the damping direction of the neoclassical flow changes depending the property of the orbits of the particles. In the limit of the $1/\nu$ regime, it is given by following equations[13],

$$G_b^{1/\nu} = \frac{1}{f_t} \left\{ \langle g_2 \rangle - \frac{3}{4} \frac{\langle B^2 \rangle}{B_{max}^2} \int_0^1 \frac{\langle g_4 \rangle}{\langle g_1 \rangle} \lambda d\lambda \right\}, \tag{2.3}$$

$$g_1 = \sqrt{1 - \lambda \frac{B}{B_{max}}}, \tag{2.4}$$

where the bracket means the surface average and f_t is the fraction of the trapped particles given by

$$f_t = 1 - \frac{3}{4} \frac{\langle B^2 \rangle}{B_{max}^2} \int_0^1 \frac{1}{\langle g_1 \rangle} \lambda d\lambda, \tag{2.5}$$

and g_2 and g_4 satisfy the magnetic differential equations of

$$\boldsymbol{B}\cdot\nabla\left(\frac{g_2}{B^2}\right)=\boldsymbol{B}\times\nabla\upsilon\cdot\nabla\left(\frac{1}{B^2}\right)\qquad g_2(B_{max})=0 \tag{2.6}$$

and

$$\boldsymbol{B}\cdot\nabla\left(\frac{g_4}{g_1}\right)=\boldsymbol{B}\times\nabla\upsilon\cdot\nabla\left(\frac{1}{g_1}\right),\qquad g_4(B_{max})=0, \tag{2.7}$$

respectively. In the limit of the plateau regime, the geometrical factor, G_b^{pl} is given by[14]

$$G_b^{pl}=\langle g_2\rangle-\sqrt{\pi}(J+\iota I)\lambda_{pl}\left\langle(\hat{\boldsymbol{n}}\cdot\nabla B)\sum_{m\neq 0\ or\ n\neq 0}\frac{1}{|m\iota+n|}\left(\frac{1}{B^2}\hat{\boldsymbol{n}}\cdot\nabla g_2\right)_{mn}\exp\imath(m\theta+n\zeta)\right\rangle \tag{2.8}$$

$$\lambda_{pl}=\frac{2\langle B^2\rangle}{\sqrt{\pi}(J+\iota I)\left\langle(\hat{\boldsymbol{n}}\cdot\nabla B)\sum_{m\neq 0\ or\ n\neq 0}\frac{1}{|m\iota+n|}\left(\frac{1}{B}\hat{\boldsymbol{n}}\cdot\nabla B\right)_{mn}\exp i(m\theta+n\zeta)\right\rangle} \tag{2.9}$$

where

$$A_{mn}=\frac{1}{(2\pi)^2}\int_0^{2\pi}d\theta\int_0^{2\pi}d\zeta A\exp i(m\theta+n\zeta). \tag{2.10}$$

Here we employed the Boozer coordinates (ψ,θ,ζ)[15], where θ and ζ denote and the poloidal and the toroidal angles, respectively. $\hat{\boldsymbol{n}}$ is the unit vector along the magnetic field, $\boldsymbol{B}$, and $2\pi I$ are the total toroidal current inside the flux surface. Since the plasma collisionality in the present study is always between the $1/\nu$ and the plateau regimes, the factor in the Pfirsch-Schlüter regime is not discussed.

In order to obtain the bootstrap current of the plasma with any collisionality between above two limits, we utilized a connection formula given by Watanabe et al.[14] for the products of G_b and L_j. In the connection formula, the collision frequency normalized by the bounce frequency, ν_*, is used as the parameter of the collisionality, which is defined by[14]

$$\nu_*=\frac{4}{3\sqrt{\pi}}\frac{f_t}{1-f_t}\frac{\lambda_{pl}}{\lambda}, \tag{2.11}$$

where λ denotes the mean free path of the particle. Although ν_* depends on the species of the particle in general, the ions and the electrons have the same value here because it is assumed that they have the same density and temperature. The limits of $\nu_*<<1$ and $\nu_*>>1$ correspond to the $1/\nu$ and the plateau collisionality regimes, respectively. Thus, the connection formula is derived so that the the products of G_b and L_j in each limit should result in those given by the asymptotic expressions. The products between the two limits are given by the combinations of the asymptotic values of G_b and L_j in the two limits

with weights depending on ν_*. The exact expression of the connection formula is given in Ref.[14].

Although L_j's also depend on the collisionality of the plasma, the variations of them in the present study are small compared with those of G_b. Hence, we concentrate on the behavior of G_b rather than the products of G_b and L_j. Figure 1 (a) and (b) shows the profiles of the geometrical factors normalized by G_b^{tok} for the $1/\nu$ and the plateau regimes in the LHD configuration, respectively. In the vacuum configuration, G_b^{pl} has negative value except the vicinity of the magnetic axis, while $G_b^{1/\nu}$ is positive in the whole region. This property makes us expect that the bootstrap current of the plasma in the plateau regime has an opposite sign of that in the $1/\nu$ regime. Thus, we investigate two sequences in raising the beta value. One is the temperature sequence where the temperature is increased with the density fixed. The other one is the density sequence where the density is increased with the temperature fixed. Here we assume that the profiles of the temperature and the density are fixed as

$$T(\psi) = T_0(1-\psi), \qquad n(\psi) = n_0(1-\psi), \tag{2.12}$$

respectively. We used $n_0 = 0.2 \times 10^{20} m^{-3}$ and $T_0 = 0.5keV$ for the temperature and the density sequences, respectively. We also assume $B_0 = 1T$ at the center of the helical coils.

The total bootstrap currents given by (2.1) in the two sequences are shown in Fig.2. The positive value in the figure corresponds to the net toroidal current flowing in the direction so as to increase the rotational transform. In the temperature sequence, the positive bootstrap current is enhanced as the beta value grows. The total current is $+101.5kA$ at $\beta_0 = 6.4\%$, where the temperature is $T_0 = 4.0keV$. Here β_0 is the beta value at the magnetic axis. On the other hand, in the density sequence, the total bootstrap current is enhanced in the positive direction up to $\beta_0 = 4\%$; however the absolute value is much less than that in the temperature sequence. The current is reduced beyond $\beta_0 = 4\%$ and becomes negative for $\beta_0 \geq 6\%$. That is, the total bootstrap current reverses the direction. The value at $\beta_0 = 6.4\%$ is $-3.8kA$, where the density is $n_0 = 1.6 \times 10^{20} m^{-3}$.

In order to know the collisionality of the plasma, we plotted ν_* in Fig.3. Since ν_* at $\beta_0 = 6.4\%$ in the temperature sequence is much less than unity, the collisionality is in the $1/\nu$ regime, and therefore, the geometrical factor given by the connection formula is almost the same as $G_b^{1/\nu}$. In this sequence, the profile of $G_b^{1/\nu}$ is insensitive to the beta

value as shown in Fig.1(a) Hence, the large positive bootstrap current flows because of the positive $G_b^{1/\nu}$ which has dominant influence in the evaluation of the bootstrap current Figure 4 shows the bootstrap current density given by eq (2.2). The current density in the temperature sequence is always positive because the contribution of G_b^{pl} is small.

On the other hand, the plasma in the density sequence becomes more collisional as beta grows and ν_* is larger than unity at $\beta_0 = 6.4\%$. Therefore, the contribution of G_b^{pl} in the geometrical factor is larger than that of $G_b^{1/\nu}$. At this beta value, G_b^{pl} is negative in the whole plasma region with comparable absolute value with $G_b^{1/\nu}$. Hence, the total bootstrap current reverses the direction due to mainly the negative G_b^{pl} for $\beta_0 \geq 6\%$. However, the effect of the change in the profile of $G_b^{1/\nu}$ cannot be neglected. As shown in Fig.4, the bootstrap current density reverses partially in the radial direction. There still exists a positive current density region in the peripheral region of the plasma in this case, although the integrated total current, I_b, is negative. Figure 1(a) shows the reduction of $G_b^{1/\nu}$ in the central region, which almost coincides with the region with the negative current density. As a result, the total bootstrap current in the density sequence reverses the direction due to not only the enhancement of the contribution of the negative G_b^{pl} but also the reduction of the positive $G_b^{1/\nu}$ in the central region.

3 Collisionality Effects on Mercier Criterion

It is known that the Mercier criterion[6, 7] strongly depends on the direction of the net toroidal current with a current density profile peaked at the magnetic axis in LHD[5]. Here we study the effects of the collisionality of the plasma on the Mercier criterion because the bootstrap current in the temperature sequence flows in the direction so as to increase the rotational transform while the current in the density sequence can flow in the opposite direction in the LHD configuration.

We evaluate D_I which is the normalized Mercier criterion so that the shear term should be $-1/4$[16]. Figure 5 shows the unstable regions against the Mercier modes. We also plot the contours of D_I, because the absolute value of D_I can be related to the global interchange modes. The global modes can be often obtained numerically beyond $D_I \simeq 0.2$[17], and

the weak interchange modes which would exist in the region $0 < D_I < 0.2$ are considered to be easily stabilized by some kinetic effects. In the temperature sequence, there exists a large unstable region in the plasma column and the value of D_I is enhanced as the beta value grows. Therefore, a considerable unstable global mode will appear even in low beta equilibria. We also see an unstable region in the density sequence. However, the largest value of D_I is 0.38, and D_I is almost less than 0.2 at the positions with $\iota = 1$, 3/4, 2/3 and 1/2, where low mode-number global modes are resonant. Hence, there would not exist an unstable global mode which leads to a catastrophic degradation of the plasma confinement, although some fluctuations may be observed.

In order to understand above properties in the Mercier stability, we focus on the rotational transform. The profile of the rotational transform changes because of two effects in the LHD equilibria carrying the bootstrap current. One is the direct change of the poloidal magnetic field generated by the bootstrap current. The other one is the diamagnetic effect related to the Shafranov shift. In Fig.6, increase of the rotational transform in the vicinity of the magnetic axis can be seen in both cases of the temperature and the density sequences at $\beta_0 = 6.4\%$ compared with that in the vacuum configuration. However, the mechanism of the increase is different. In the temperature sequence, the rotational transform is increased directly by the positive bootstrap current density shown in Fig.4. Hence, it is larger than that in the vacuum configuration in the whole plasma region. On the other hand, in the density sequence, the bootstrap current density is negative for $\psi \leq 0.5$ while it is positive in other region as shown in Fig.4. This property is not reflected directly in the profile of the rotational transform, because the rotational transform at the magnetic axis is lifted up and the one in the peripheral region is pulled down as shown in Fig.6. It can be understood by taking account of the diamagnetic effects attributed to the Pfirsch-Schlüter current. The Shafranov shift of the magnetic axis, which is brought by the Pfirsch-Schlüter current, is proportional to the inverse of the square of the rotational transform at the magnetic axis in the large aspect ratio limit. The bootstrap current itself decreases the rotational transform in the density sequence. The decrease results in the large Shafranov shift as shown in Fig.7, where the shifts of the magnetic axis normalized by the average minor radius are plotted. As is seen in the currentless equilibria in Ref.[5], the deformation of the flux surfaces accompanied by the Shafranov shift brings the increase of the rotational

transform at the magnetic axis and the decrease at the peripheral region so as to produce a local minimum in the profile. Therefore, the large Shafranov shift in the density sequence enhances the increase of the rotational transform at the magnetic axis which is superior to the direct decrease due to the bootstrap current itself. In this case, the decrease of the rotational transform at the peripheral region results in the enhancement of the magnetic shear which has stabilizing contribution to the Mercier mode. In the temperature sequence, the Shafranov shift is smaller than that in the density sequence because of the increase of the rotational transform by the bootstrap current, and the magnetic shear is reduced.

The large Shafranov shift enhances the magnetic well. We plot the magnetic well depth defined by $[V'(0) - V'(\psi)]/V'(0)$ in Fig.8, where V is the volume of the flux tube and the prime denotes the derivative with respect to ψ. The positive gradient of the profiles corresponds to the magnetic well. In the vacuum configuration, there is no magnetic well region. At $\beta_0 = 6.4\%$, the well region spreads at $0 \leq \psi \leq 0.46$ and the gradient becomes steep in the density sequence. The weak shear region located around $\psi \simeq 0.37$ seen in Fig.6 is covered by the well region. On the contrary, the well depth is suppressed due to the small Shafranov shift in the temperature sequence.

As a result, in the density sequence, both the enhancements of the magnetic well and the magnetic shear stabilize the Mercier mode owing to the decrease in the rotational transform by the bootstrap current. Furthermore, the second stability region for the Mercier criterion appears at $\beta_0 > 5.8\%$. In the currentless case with the same pressure profile, the second stability is also found, however it appears only beyond $\beta_0 = 8\%$[5]. At $\beta_0 = 6\%$ in the density sequence, the total bootstrap current is almost zero as shown in Fig.2. Nevertheless, the equilibrium is already in the second stability region, while the currentless equilibrium at the same beta has a slightly unstable region in the plasma column. This is because the bootstrap current density locally reverses the direction near the magnetic axis although the integrated total current in the whole plasma is almost zero. Therefore, the magnetic well and shear are enhanced by the reduction of the rotational transform compared with the corresponding currentless equilibrium, and stabilize the Mercier modes completely.

4 Concluding Remarks

We investigated the dependence of the Mercier stability on the collisionality of the LHD plasma through the change in the direction of the bootstrap current. Here we noticed the behavior of the geometrical factor, which dominates the property of the bootstrap current. The positive value of the geometrical factor corresponds to the direction of the bootstrap current increasing the rotational transform. In vacuum configuration of the LHD, the geometrical factor in the limit of the $1/\nu$ collisionality regime, $G_b^{1/\nu}$, is positive and that in the limit of the plateau regime, G_b^{pl}, is negative. We utilized a connection formula in the expression of the bootstrap current to evaluate the current continuously between the $1/\nu$ and the plateau regimes. In this paper, we considered two cases of the temperature and the density sequences in raising the beta value.

In the temperature sequence, we raised the beta value by increasing the temperature with the density fixed. Then, the plasma becomes less collisional as beta grows, and the geometrical factor is dominated by $G_b^{1/\nu}$. In this case, the profile of $G_b^{1/\nu}$ hardly depends on the beta value. Hence, we obtained a significant bootstrap current flowing in the direction so as to increase the rotational transform. In this case, the Mercier stability is deteriolated.

On the contrary, in the density sequence, we raised the beta value by increasing the density with the fixed temperature. Then, the plasma approaches to the plateau regime. In the geometrical factor in the connection formula, the contribution of G_b^{pl} becomes dominant. G_b^{pl} becomes more negative as beta grows. It is found that the total bootstrap current reverses the direction and flows in the direction so as to decrease the rotational transform at $\beta \geq 6\%$. In this case, the current density partially reverses the direction in the central region, while the current density increasing the rotational transform still exists in the peripheral region. In the equilibrium, the enlarged Shafranov shift by the reduction of the rotational transform enhances the stabilizing effects of the magnetic shear and the magnetic well. Hence, the Mercier stability is improved, and a second stability region appears at lower beta value than that in the currentless equilibrium sequence with the same pressure profile. Thus, the beta value should be raised by increasing the density rather than the temperature to obtain a stable plasma in high-beta experiments in LHD.

In the reverse of the direction of the bootstrap current, the reduction of the positive $G_b^{1/\nu}$ is seen in the central region. The region of the reduction almost coincides with the region with the reversed current density. It implies that the change in the profile of $G_b^{1/\nu}$ advances the reverse of the bootstrap current. Consequently, the plasma does not need to enter the plateau collisionality regime completely to reverse the direction of the current. Indeed, we found the reverse at ν_* less than 10 which is not very much larger than unity. It is considered that the reduction of $G_b^{1/\nu}$ results from the large Shafranov shift, because $G_b^{1/\nu}$ is sensitive to the change in the magnetic configuration. Watanabe et al.[10] showed that the vertical elongation of the plasma shape reduces the bootstrap current in $1/\nu$ regime, and Ichiguchi et al.[18] showed the reverse of the direction in the case of the helical axis configuration generated by unbalancing the helical coil currents. Hence, the direction of the bootstrap current will reverse more easily, and therefore, more stable path to a high-beta equilibria would be found, by combining the collisionality effect with the geometrical change in the magnetic configuration.

Acknowledgements

The auther would like to thank to Prof.M.Okamoto, Dr.N.Nakajima and Dr.K.Y.Watanabe for their fruitful discussions.

References

[1] Shaing K C and Callen J D 1983 *Phys. Fluids* **26** 3315.

[2] Shaing K C, Carreras B A, Dominguez N, Lynch V E and Tolliver J S 1989 *Phys. Fluids* **B1** 1663.

[3] Nakajima N, Okamoto M, Todoroki J, Nakamura Y and Wakatani M 1989 *Nucl. Fusion* **29** 605.

[4] Nakajima N and Okamoto M 1992 *J. Phys. Soc. Jpn.* **61** 833.

[5] Ichiguchi K, Nakajima N, Okamoto M, Nakamura Y and Wakatani M 1993 *Nucl. Fusion* **33** 481.

[6] Mercier C 1962 *Nucl. Fusion Suppl.* Pt.2, 801.

[7] Johnson J L and Greene J M 1967 *Plasma Phys.* **9** 611.

[8] Iiyoshi A, Fujiwara M, Motojima O, Oyabu N and Yamazaki K 1990 *Fusion Tech.* **17** 169.

[9] Iiyoshi A and Yamazaki K 1995 *Phys. Plasmas* **2** 2349.

[10] Watanabe K, Nakajima N, Okamoto M, Nakamura Y and Wakatoni M 1992 *Nucl. Fusion* **32** 1499.

[11] Hirshman S P, Van Rij W I and Merkel P 1986 *Comp. Phys. Comm.* **43** 143.

[12] Nakajima N, Okamoto M and Fujiwara M 1992 *Kakuyugo Kenkyu* **68** 503.

[13] Nakajima N and Okamoto M 1992 *J. Phys. Soc. Jpn.* **61** 833.

[14] Watanabe K, Nakajima N, Okamoto M, Yamazaki K, Nakamura Y and Wakatani M 1995 *Nucl. Fusion* **35** 335.

[15] Boozer A H 1982 *Phys. Fluids* **25** 520.

[16] Glasser A H, Greene J M and Johnson J L 1975 *Phys. Fluids* **18** 875.

[17] Nakamura Y, Ichiguchi K, Wakatani M and Johnson J L 1989 *J. Phys. Soc. Jpn.* **58** 3157.

[18] Ichiguchi K, Nakajima N and Okamoto M '*Bootstrap Current in Large Helical Device with Unbalanced Helical-Coil Currents*', (in preperation).

Figure Captions

Fig.1 Profiles of normalized geometrical factors in the limit of (a) $1/\nu$ and (b) plateau regimes in LHD with $B_0 = 1T$. Solid lines show the values in the vacuum configuration. Dashed and dot-dashed lines show the values at $\beta_0 = 6.4\%$ for $T_0 = 4keV$, $n_0 = 0.2 \times 10^{20} m^{-3}$ in the temperature sequence and $T_0 = 0.5keV$, $n = 1.6 \times 10^{20} m^{-3}$ in the density sequence.

Fig.2 Total bootstrap currents versus β_0 in the temperature sequence (dashed line) and the density sequence (dot-dashed line).

Fig.3 Profiles of normalized collision frequency. Dashed and dot-dashed lines correspond to the cases of the same lines in Fig.1, respectively.

Fig.4 Profiles of the bootstrap current density. Dashed and dot-dashed lines correspond to the cases of the same lines in Fig.1, respectively.

Fig.5 Mercier unstable regions for (a) temperature sequence and (b) density sequence in the (β_0, ψ) plane. Shaded regions show unstable regions. Solid lines in these regions are the contours of the level surface of D_I which differ by $\Delta D_I = 0.2$. In (a) the contours with $D_I > 8.0$ are not plotted because they are too dense. Dot-dashed line shows the boundary between the magnetic well and hill regions. Dashed lines indicate the positions of the rational surfaces corresponding to $\iota = 1$, 3/4, 2/3 and 1/2 from right to left.

Fig.6 Rotational transform profiles. Solid, dashed and dot-dashed lines correspond to the cases of the same lines in Fig.1, respectively.

Fig.7 Shafranov shift versus β_0 in the temperature sequence (dashed line) and the density sequence (dot-dashed line).

Fig.8 Profiles of magnetic well depth. Solid, dashed and dot-dashed lines correspond to the cases of the same lines in Fig.1, respectively.

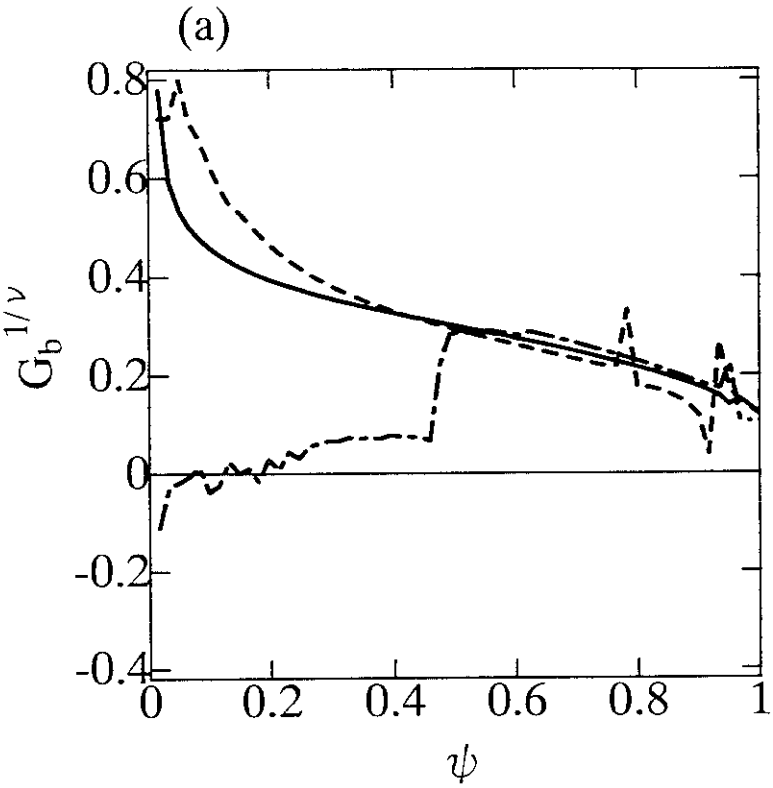
(a)
0.8
0.6
0.4
0.2
0
-0.2
-0.4
$G_b^{1/\nu}$
0
0.2
0.4
0.6
0.8
1
ψ

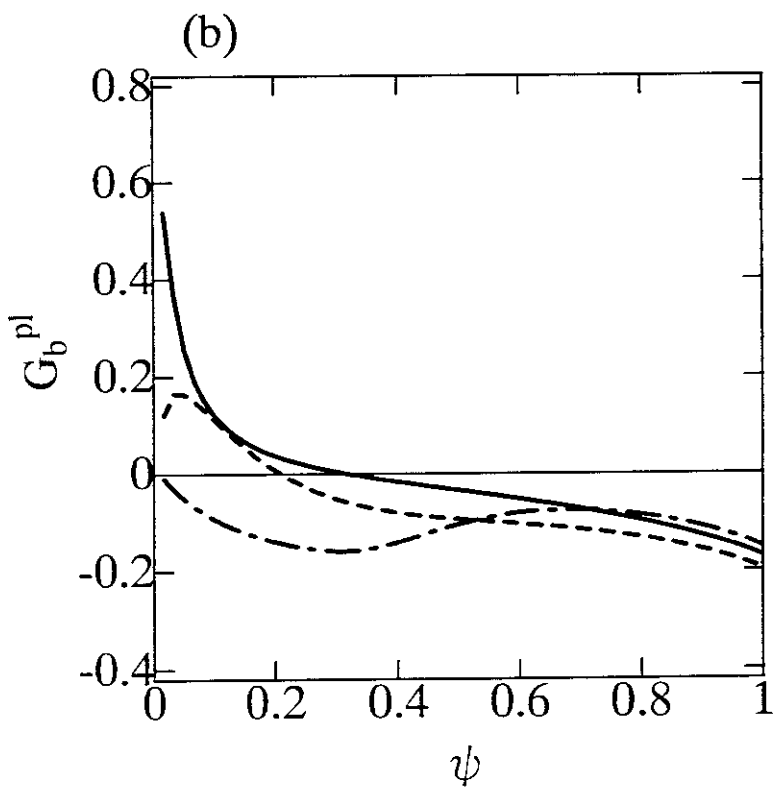
(b)
0.8
0.6
0.4
0.2
0
-0.2
-0.4
G_b^{pl}
0
0.2
0.4
0.6
0.8
1
ψ

Fig.1

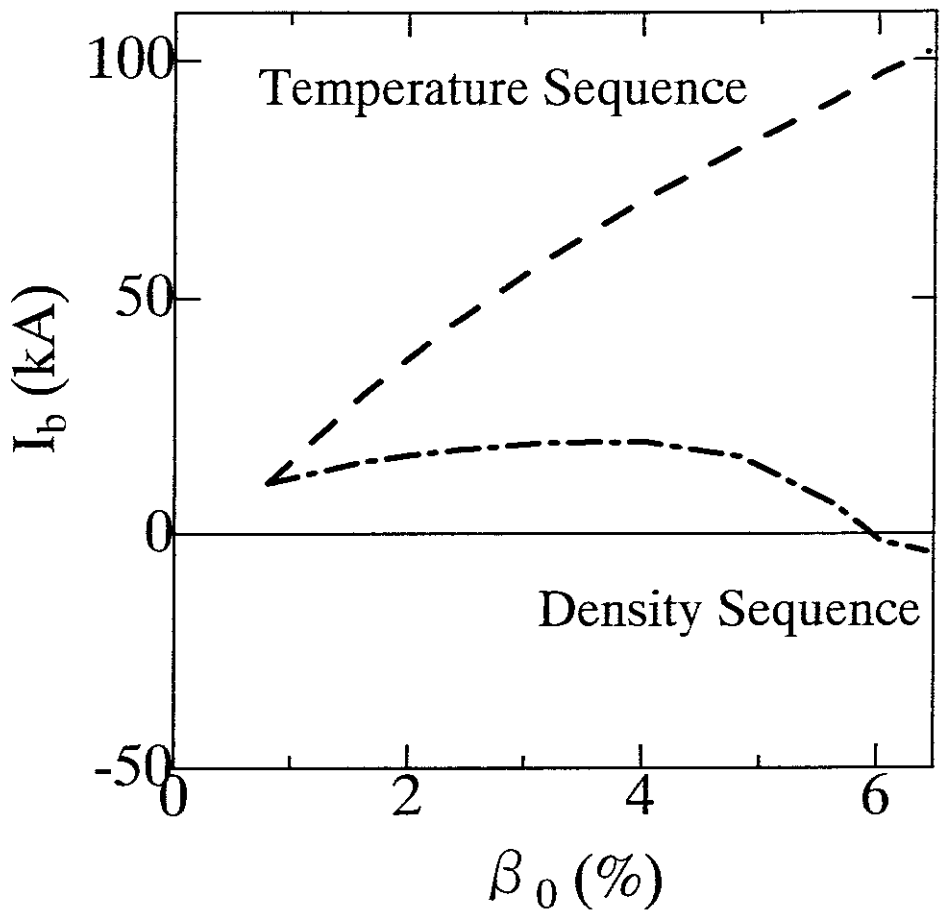
100
50
0
-50
0
2
4
6
Temperature Sequence
Density Sequence
I_b (kA)
β_0 (%)

Fig.2

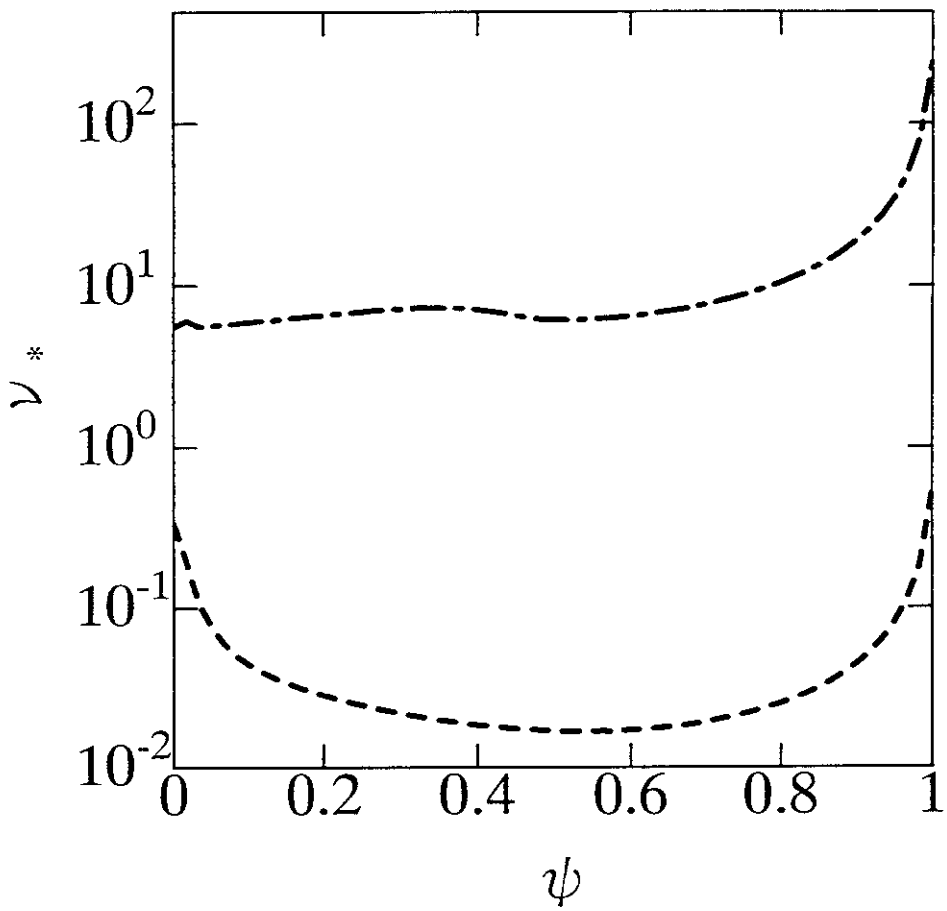

Fig.3

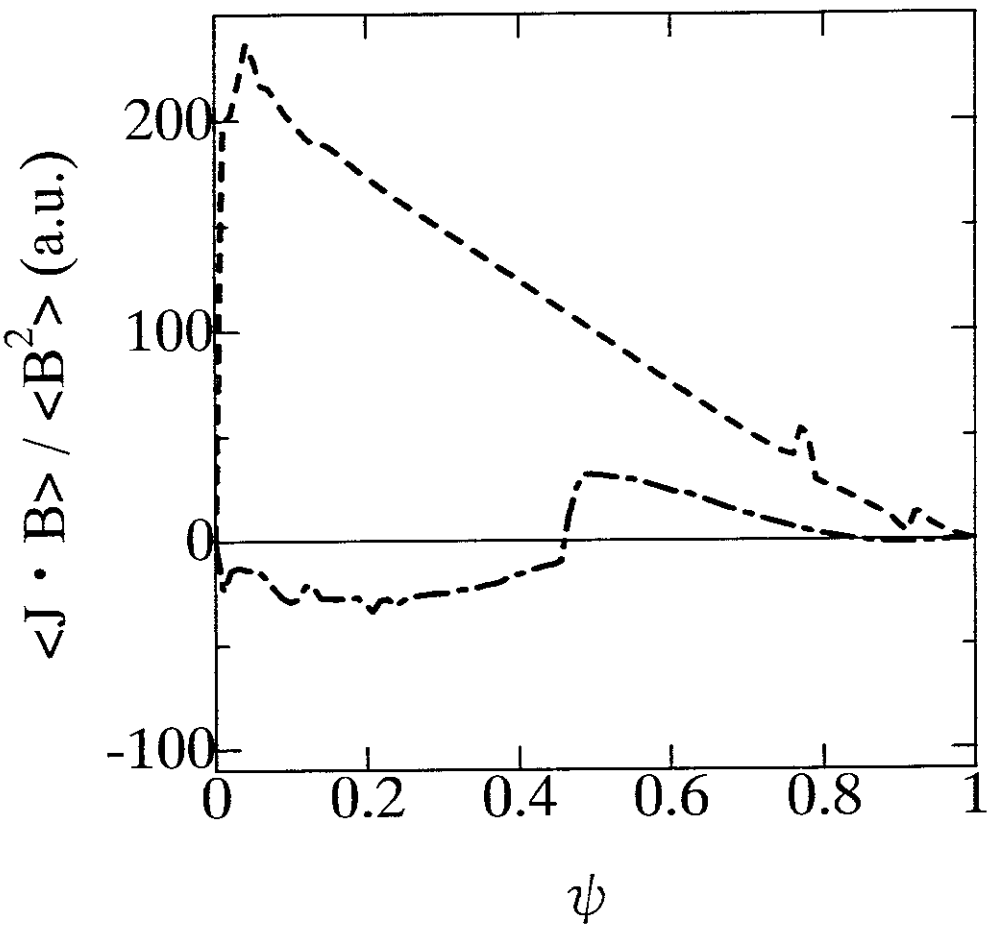
200
100
0
-100
0
0.2
0.4
0.6
0.8
1
ψ
$\langle J \cdot B \rangle / \langle B^2 \rangle$ (a.u.)

Fig.4

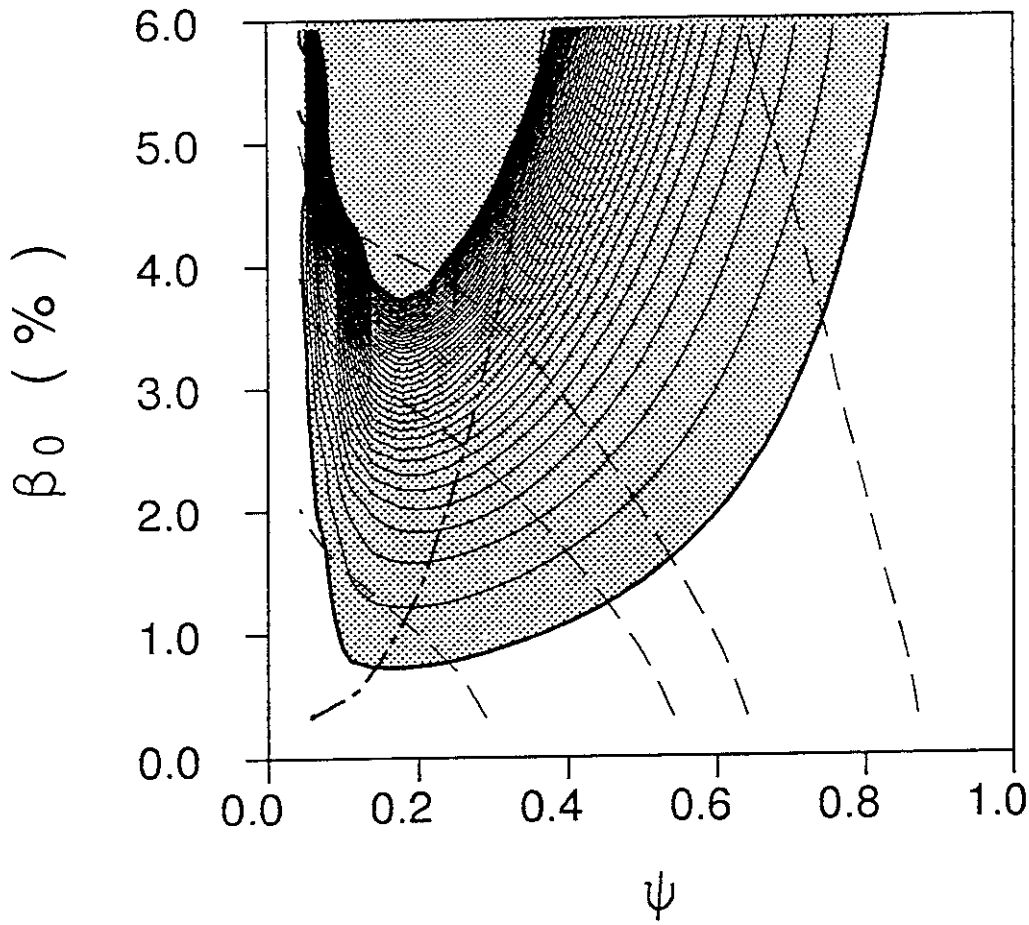

Fig.5 (a)

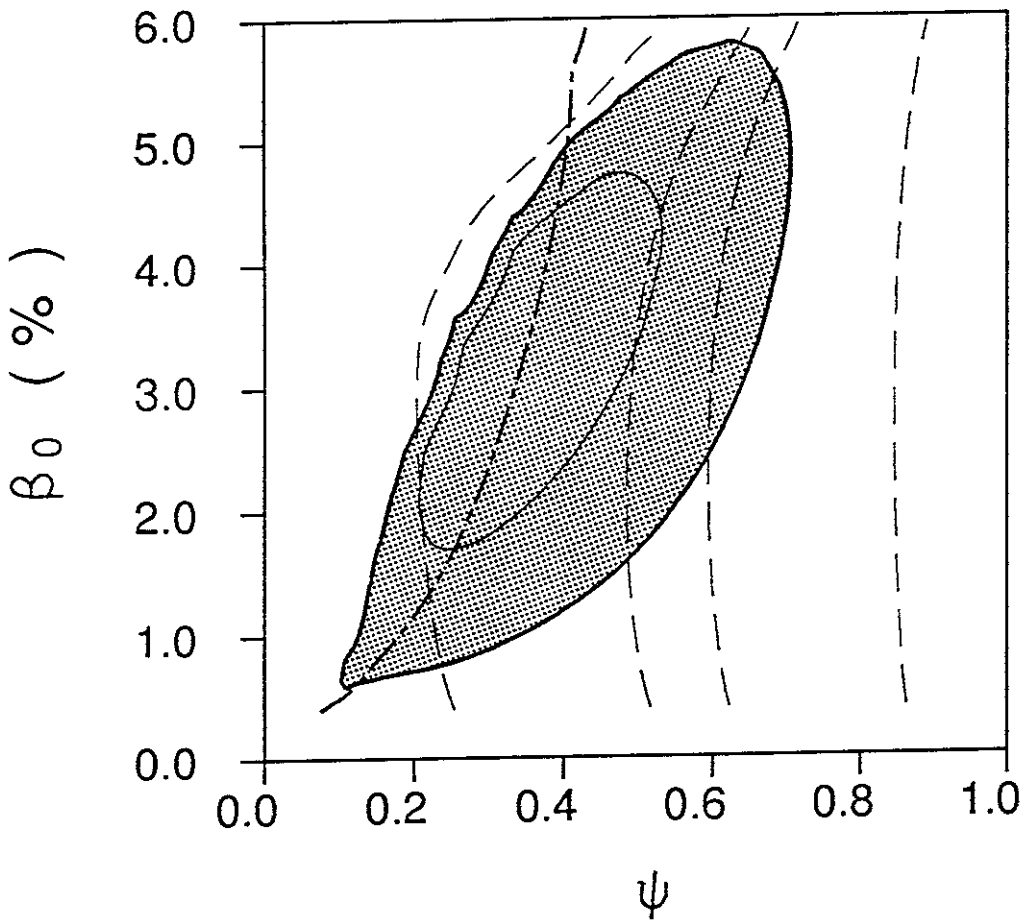

Fig.5 (b)

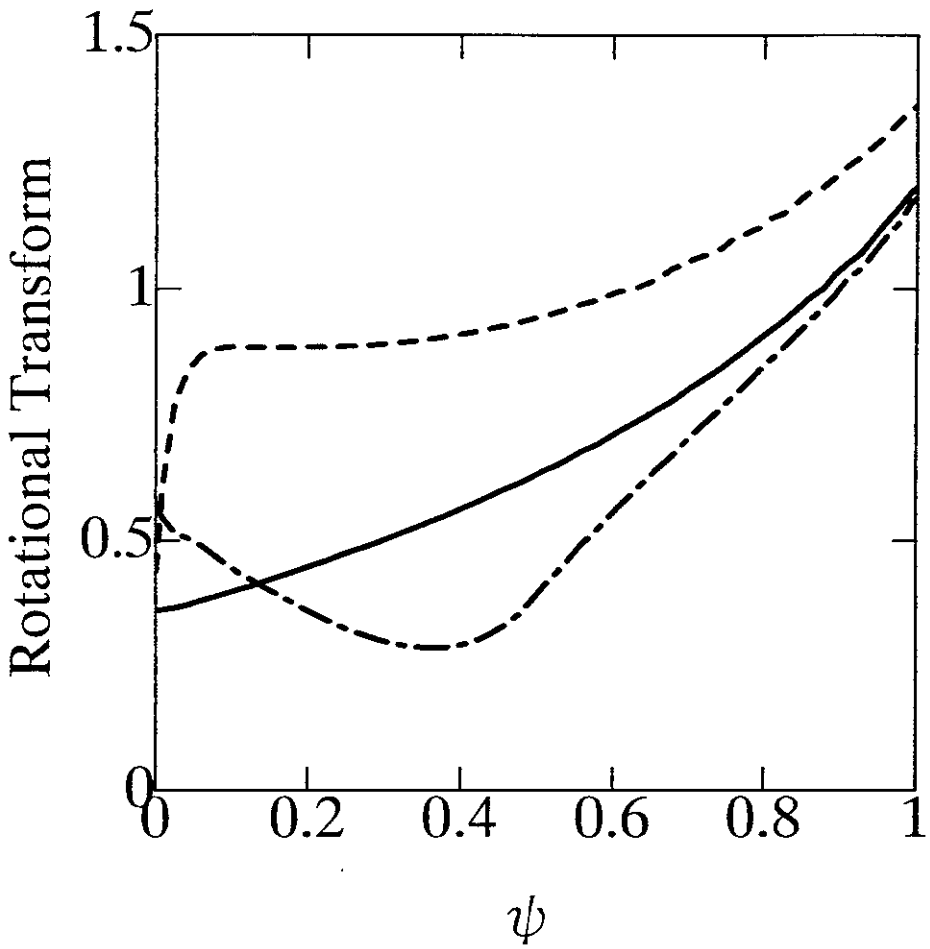

Fig.6

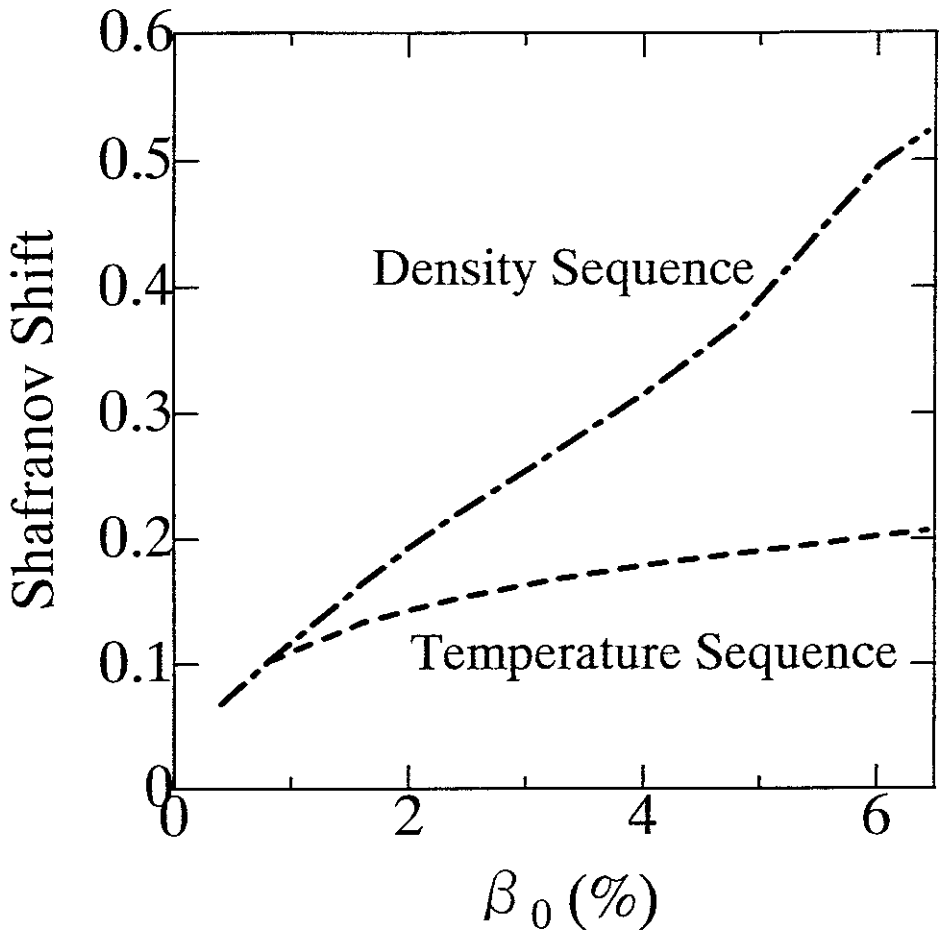
0.6
0.5
0.4
0.3
0.2
0.1
0
Shafranov Shift
Density Sequence
Temperature Sequence
0
2
4
6
β_0 (%)

Fig.7

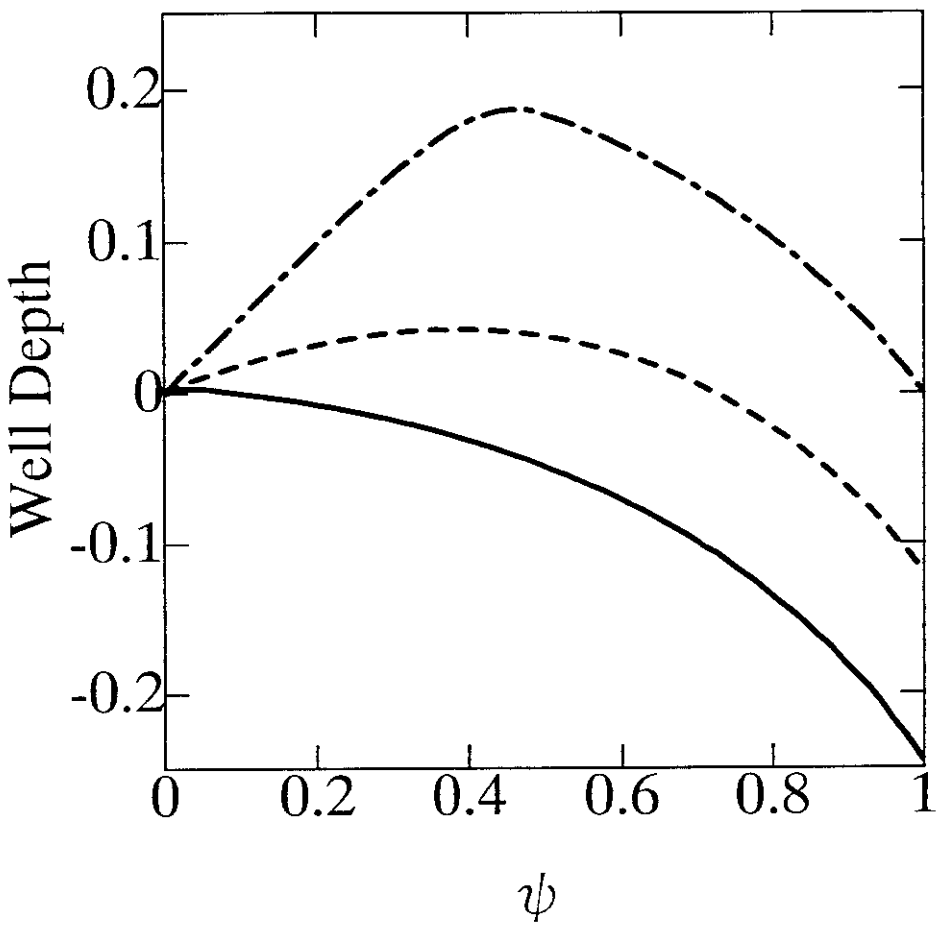

Fig.8

Recent Issues of NIFS Series

NIFS-441 O. Kaneko, Y. Takeiri, K. Tsumori, Y. Oka, M. Osakabe, R. Akiyama, T. Kawamoto, E. Asano and T. Kuroda,
Development of Negative-Ion-Based Neutral Beam Injector for the Large Helical Device; Sep. 1996 (IAEA-CN-64/GP-9)

NIFS-442 K. Toi, K.N. Sato, Y. Hamada, S. Ohdachi, H. Sakakita, A. Nishizawa, A. Ejiri, K. Narihara, H. Kuramoto, Y. Kawasumi, S. Kubo, T. Seki, K. Kitachi, J. Xu, K. Ida, K. Kawahata, I. Nomura, K. Adachi, R. Akiyama, A. Fujisawa, J. Fujita, N. Hiraki, S. Hidekuma, S. Hirokura, H. Idei, T. Ido, H. Iguchi, K. Iwasaki, M. Isobe, O. Kaneko, Y. Kano, M. Kojima, J. Koog, R. Kumazawa, T. Kuroda, J. Li, R. Liang, T. Minami, S. Morita, K. Ohkubo, Y. Oka, S. Okajima, M. Osakabe, Y. Sakawa, M. Sasao, K. Sato, T. Shimpo, T. Shoji, H. Sugai, T. Watari, I. Yamada and K. Yamauti,
Studies of Perturbative Plasma Transport, Ice Pellet Ablation and Sawtooth Phenomena in the JIPP T-IIU Tokamak; Sep. 1996 (IAEA-CN-64/A6-5)

NIFS-443 Y. Todo, T. Sato and The Complexity Simulation Group,
Vlasov-MHD and Particle-MHD Simulations of the Toroidal Alfvén Eigenmode; Sep. 1996 (IAEA-CN-64/D2-3)

NIFS-444 A. Fujisawa, S. Kubo, H. Iguchi, H. Idei, T. Minami, H. Sanuki, K. Itoh, S. Okamura, K. Matsuoka, K. Tanaka, S. Lee, M. Kojima, T.P. Crowley, Y. Hamada, M. Iwase, H. Nagasaki, H. Suzuki, N. Inoue, R. Akiyama, M. Osakabe, S. Morita, C. Takahashi, S. Muto, A. Ejiri, K. Ida, S. Nishimura, K. Narihara, I. Yamada, K. Toi, S. Ohdachi, T. Ozaki, A. Komori, K. Nishimura, S. Hidekuma, K. Ohkubo, D.A. Rasmussen, J.B. Wilgen, M. Murakami, T. Watari and M. Fujiwara,
An Experimental Study of Plasma Confinement and Heating Efficiency through the Potential Profile Measurements with a Heavy Ion Beam Probe in the Compact Helical System; Sep. 1996 (IAEA-CN-64/C1-5)

NIFS-445 O. Motojima, N. Yanagi, S. Imagawa, K. Takahata, S. Yamada, A. Iwamoto, H. Chikaraishi, S. Kitagawa, R. Maekawa, S. Masuzaki, T. Mito, T. Morisaki, A. Nishimura, S. Sakakibara, S. Satoh, T. Satow, H. Tamura, S. Tanahashi, K. Watanabe, S. Yamaguchi, J. Yamamoto, M.Fujiwara and A. Iiyoshi,
Superconducting Magnet Design and Construction of LHD; Sep. 1996 (IAEA-CN-64/G2-4)

NIFS-446 S. Murakami, N. Nakajima, S. Okamura, M. Okamoto and U. Gasparino,
Orbit Effects of Energetic Particles on the Reachable β–Value and the Radial Electric Field in NBI and ECR Heated Heliotron Plasmas; Sep. 1996 (IAEA-CN-64/CP -6) Sep. 1996

NIFS-447 K. Yamazaki, A. Sagara, O. Motojima, M. Fujiwara, T. Amano, H. Chikaraishi, S. Imagawa, T. Muroga, N. Noda, N. Ohyabu, T. Satow, J.F. Wang, K.Y. Watanabe, J. Yamamoto , H. Yamanishi, A. Kohyama, H. Matsui, O. Mitarai, T. Noda, A.A. Shishkin, S. Tanaka and T. Terai
Design Assessment of Heliotron Reactor; Sep. 1996 (IAEA-CN-64/G1-5)

NIFS-448 M. Ozaki, T. Sato and the Complexity Simulation Group,
Interactions of Convecting Magnetic Loops and Arcades; Sep. 1996

NIFS-449 T. Aoki,
Interpolated Differential Operator (IDO) Scheme for Solving Partial Differential Equations; Sep. 1996

NIFS-450 D. Biskamp and T. Sato,
Partial Reconnection in the Sawtooth Collapse; Sep. 1996

NIFS-451 J. Li, X. Gong, L. Luo, F.X. Yin, N. Noda, B. Wan, W. Xu, X. Gao, F. Yin, J.G. Jiang, Z. Wu., J.Y. Zhao, M. Wu, S. Liu and Y. Han,
Effects of High Z Probe on Plasma Behavior in HT-6M Tokamak; Sep. 1996

NIFS-452 N. Nakajima, K. Ichiguchi, M. Okamoto and R.L. Dewar,
Ballooning Modes in Heliotrons/Torsatrons; Sep. 1996 (IAEA-CN-64/D3-6)

NIFS-453 A. Iiyoshi,
Overview of Helical Systems; Sep. 1996 (IAEA-CN-64/O1-7)

NIFS-454 S. Saito, Y. Nomura, K. Hirose and Y.H. Ichikawa,
Separatrix Reconnection and Periodic Orbit Annihilation in the Harper Map; Oct. 1996

NIFS-455 K. Ichiguchi, N. Nakajima and M. Okamoto,
Topics on MHD Equilibrium and Stability in Heliotron / Torsatron; Oct. 1996

NIFS-456 G. Kawahara, S. Kida, M. Tanaka and S. Yanase,
Wrap, Tilt and Stretch of Vorticity Lines around a Strong Straight Vortex Tube in a Simple Shear Flow; Oct. 1996

NIFS-457 K. Itoh, S.- I. Itoh, A. Fukuyama and M. Yagi,
Turbulent Transport and Structural Transition in Confined Plasmas; Oct. 1996

NIFS-458 A. Kageyama and T. Sato,
Generation Mechanism of a Dipole Field by a Magnetohydrodynamic Dynamo; Oct. 1996

NIFS-459 K. Araki, J. Mizushima and S. Yanase,
The Non-axisymmetric Instability of the Wide-Gap Spherical Couette Flow; Oct. 1996

NIFS-460 Y. Hamada, A. Fujisawa, H. Iguchi, A. Nishizawa and Y. Kawasumi,
A Tandem Parallel Plate Analyzer; Nov. 1996

NIFS-461 Y. Hamada, A. Nishizawa, Y. Kawasumi, A. Fujisawa, K. Narihara, K. Ida, A. Ejiri, S. Ohdachi, K. Kawahata, K. Toi, K. Sato, T. Seki, H. Iguchi, K. Adachi, S. Hidekuma,

S.Hirokura, K. Iwasaki, T. Ido, M. Kojima, J. Koong, R. Kumazawa, H. Kuramoto, T. Minami, I. Nomura, H. Sakakita, M. Sasao, K. N. Sato, T. Tsuzuki, J. Xu, I. Yamada and T. Watari,
Density Fluctuation in JIPP T-IIU Tokamak Plasmas Measured by a Heavy Ion Beam Probe; Nov. 1996

NIFS-462 N. Katsuragawa, H. Hojo and A. Mase,
Simulation Study on Cross Polarization Scattering of Ultrashort-Pulse Electromagnetic Waves; Nov. 1996

NIFS-463 V. Voitsenya, V. Konovalov, O. Motojima, K. Narihara, M. Becker and B. Schunke,
Evaluations of Different Metals for Manufacturing Mirrors of Thomson Scattering System for the LHD Divertor Plasma; Nov. 1996

NIFS-464 M. Pereyaslavets, M. Sato, T. Shimozuma, Y. Takita, H. Idei, S. Kubo, K. Ohkubo and K. Hayashi,
Development and Simulation of RF Components for High Power Millimeter Wave Gyrotrons; Nov. 1996

NIFS-465 V.S. Voitsenya, S. Masuzaki, O. Motojima, N. Noda and N. Ohyabu,
On the Use of CX Atom Analyzer for Study Characteristics of Ion Component in a LHD Divertor Plasma; Dec. 1996

NIFS-466 H. Miura and S. Kida,
Identification of Tubular Vortices in Complex Flows; Dec. 1996

NIFS-467 Y. Takeiri, Y. Oka, M. Osakabe, K. Tsumori, O. Kaneko, T. Takanashi, E. Asano, T. Kawamoto, R. Akiyama and T. Kuroda,
Suppression of Accelerated Electrons in a High-current Large Negative Ion Source; Dec. 1996

NIFS-468 A. Sagara, Y. Hasegawa, K. Tsuzuki, N. Inoue, H. Suzuki, T. Morisaki, N. Noda, O. Motojima, S. Okamura, K. Matsuoka, R. Akiyama, K. Ida, H. Idei, K. Iwasaki, S. Kubo, T. Minami, S. Morita, K. Narihara, T. Ozaki, K. Sato, C. Takahashi, K. Tanaka, K. Toi and I. Yamada,
Real Time Boronization Experiments in CHS and Scaling for LHD; Dec. 1996

NIFS-469 V.L. Vdovin, T.Watari and A. Fukuyama,
3D Maxwell-Vlasov Boundary Value Problem Solution in Stellarator Geometry in Ion Cyclotron Frequency Range (final report); Dec. 1996

NIFS-470 N. Nakajima, M. Yokoyama, M. Okamoto and J. Nührenberg,
Optimization of M=2 Stellarator; Dec. 1996

NIFS-471 A. Fujisawa, H. Iguchi, S. Lee and Y. Hamada,
Effects of Horizontal Injection Angle Displacements on Energy Measurements with Parallel Plate Energy Analyzer; Dec. 1996

NIFS-472 R. Kanno, N. Nakajima, H. Sugama, M. Okamoto and Y. Ogawa,

Effects of Finite-β and Radial Electric Fields on Neoclassical Transport in the Large Helical Device; Jan. 1997

NIFS-473 S. Murakami, N. Nakajima, U. Gasparino and M. Okamoto,
Simulation Study of Radial Electric Field in CHS and LHD; Jan. 1997

NIFS-474 K. Ohkubo, S. Kubo, H. Idei, M. Sato, T. Shimozuma and Y. Takita,
Coupling of Tilting Gaussian Beam with Hybrid Mode in the Corrugated Waveguide; Jan. 1997

NIFS-475 A. Fujisawa, H. Iguchi, S. Lee and Y. Hamada,
Consideration of Fluctuation in Secondary Beam Intensity of Heavy Ion Beam Prove Measurements; Jan. 1997

NIFS-476 Y. Takeiri, M. Osakabe, Y. Oka, K. Tsumori, O. Kaneko, T. Takanashi, E. Asano, T. Kawamoto, R. Akiyama and T. Kuroda,
Long-pulse Operation of a Cesium-Seeded High-Current Large Negative Ion Source; Jan. 1997

NIFS-477 H. Kuramoto, K. Toi, N. Haraki, K. Sato, J. Xu, A. Ejiri, K. Narihara, T. Seki, S. Ohdachi, K. Adati, R. Akiyama, Y. Hamada, S. Hirokura, K. Kawahata and M. Kojima,
Study of Toroidal Current Penetration during Current Ramp in JIPP T-IIU with Fast Response Zeeman Polarimeter; Jan. 7, 1997

NIFS-478 H. Sugama and W. Horton,
Neoclassical Electron and Ion Transport in Toroidally Rotating Plasmas; Jan. 1997

NIFS-479 V.L. Vdovin and I.V. Kamenskij,
3D Electromagnetic Theory of ICRF Multi Port Multi Loop Antenna; Jan. 1997

NIFS-480 W.X. Wang, M. Okamoto, N. Nakajima, S Murakami and N. Ohyabu,
Cooling Effect of Secondary Electrons in the High Temperature Divertor Operation; Feb. 1997

NIFS-481 K. Itoh, S.-I. Itoh, H. Soltwisch and H.R. Koslowski,
Generation of Toroidal Current Sheet at Sawtooth Crash; Feb. 1997

NIFS-482 K. Ichiguchi,
Collisionality Dependence of Mercier Stability in LHD Equilibria with Bootstrap Currents; Feb. 1997